Supplementary Information

Tailoring Re-Loaded Core-Shell Ni Constructions Embedded in Mesoporous Silica for the Selective Transformation of Levulinic Acid into γ-Valerolactone

Yupawan Maneewong[a+], Pratikkumar Lakhani[a+], Sakhon Ratchahat[a], Chularat Sakdaronnarong[a], Wanwisa Limphirat[b,c], Suttichai Assabumrungrat[d,e], Kittisak Choojun[f], Tawan Sooknoi[e], Keiichi Tomishige[g], and Atthapon Srifa[a,*]

[a] Department of Chemical Engineering, Faculty of Engineering, Mahidol University, Nakhon Pathom 73170, Thailand

[b] Synchrotron Light Research Institute, Nakhon Ratchasima, 30000, Thailand

[c] Department of Chemical Engineering, Faculty of Engineering, Chulalongkorn University, Bangkok 10330, Thailand

[d] Center of Excellence on Catalysis and Catalytic Reaction Engineering, Department of Chemical Engineering, Faculty of Engineering, Chulalongkorn University, Bangkok 10330, Thailand

[e] Bio-Circular-Green-economy Technology & Engineering Center, BCGeTEC, Faculty of Engineering, Chulalongkorn University, Bangkok 10330, Thailand

[f] Department of Chemistry, Faculty of Science, King Mongkut's Institute of Technology Ladkrabang, Chalongkrung Road, Ladkrabang, Bangkok 10520, Thailand

[g] Department of Applied Chemistry, School of Engineering, Tohoku University, 6-6-07 Aoba, Aramaki, Aoba-ku, Sendai, 980-8579, Japan,

[+]Y. Maneewong and P. Lakhani contributed equally to this work.
* To whom correspondence should be addressed.
Tel.: +66(0)2 889-2138 ext. 6101-3; Fax: +66(0)2 889-2138 ext. 6129
Email address: atthapon.sri@mahidol.edu (A. Srifa)

Entry	Caption	Page No.
1	General information of materials	**S3**
2	Characterization techniques information	**S3-S4**
Table S1	Summary of the XPS results obtained from the reduced Ni based catalysts.	**S5**
Table S2	Summary of the XPS results obtained from the reduced Ni and Ni-Re based core-shell catalysts.	**S6**
Table S3	Summary of Ni composition (%) by LCF fitting from XANES data obtained from the reduced Ni based catalysts	**S7**
Table S4	Catalytic performance comparison of Ni-based catalysts for levulinic acid (LA) hydrogenation to γ-valerolactone (GVL), highlighting LA conversion and GVL yield.	**S8**
Table S5	Summary of the XPS results obtained from the used catalysts.	**S9**
Fig. S1	(a to d) high-resolution TEM (HR-TEM) images and (a-i to d-i) diffraction pattern of the reduced (a and a-i) Ni-CS, (b and b-i) Ni-IM-mSiO_2, (c and c-i) Ni-IM-SiO_2, and (d and d-i) Ni-IM-MCM-41 catalysts, respectively.	**S10**
Fig. S2	(a to d) Field Emission Scanning Electron Microscope (FE-SEM) images of the calcined (a) Ni-CS, (b) Ni-IM-mSiO_2, (c) Ni-IM-SiO_2, and (d) Ni-IM-MCM-41 catalysts.	**S11**
Fig. S3	X-ray photoelectron spectroscopy (XPS) Ni 2*p* spectra of reduced and passivated Ni-CS, Ni-IM-mSiO_2, Ni-IM-SiO_2, and Ni-IM-MCM-41 catalysts.	**S12**
Fig. S4	(a) N_2 adsorption-desorption isotherms and (b) pore size distribution derived from the BJH model for the calcined Ni-CS $Ni_{12}Re_{0.78}$-CS, $Ni_{12}Re_{0.93}$-CS, $Ni_{12}Re_{1.63}$-CS, and $Ni_{12}Re_{1.80}$-CS catalysts.	**S13**
Fig. S5	(a to d) Field Emission Scanning Electron Microscope (FE-SEM) images of the calcined (a) Ni-CS (b) $Ni_{12}Re_{0.78}$-CS, (c) $Ni_{12}Re_{0.93}$-CS, (d) $Ni_{12}Re_{1.63}$-CS, and (e) $Ni_{12}Re_{1.80}$-CS catalysts.	**S14**
Fig. S6	(a) Ni 2*p* and (b) Re 4*f* XPS spectra of reduced and passivated Ni-CS, $Ni_{12}Re_{0.78}$-CS, $Ni_{12}Re_{0.93}$-CS, $Ni_{12}Re_{1.63}$-CS, and $Ni_{12}Re_{1.80}$-CS catalysts.	**S15**
Fig. S7	Reusability data of $Ni_{12}Re_{1.63}$-CS catalyst	**S16**
Fig. S8	TEM image of used $Ni_{12}Re_{1.63}$-CS catalyst	**S17**
Fig. S9	XRD comparison of reduced and used $Ni_{12}Re_{1.63}$-CS catalyst	**S18**
Fig. S10	X-ray photoelectron spectroscopy (XPS) (a) Ni 2*p* and (b) Re 4*f* spectra of used $Ni_{12}Re_{1.63}$-CS catalyst	**S19**
Fig. S11	Normalized (a) Ni K- and (b) Re L_3-edges XANES spectra of used $Ni_{12}Re_{1.63}$-CS catalyst	**S20**
Fig. S12	EXAFS spectra at the (a) Ni K-edge and (b) Re L_3-edge for the used $Ni_{12}Re_{1.63}$-CS catalyst	**S21**
Fig. S13	TGA comparison of reduced and used $Ni_{12}Re_{1.63}$-CS catalyst	**S22**

1. General information of materials

MCM-41 was obtained from ACS Material LLC with a purity of 99%. Nickel(II) nitrate hexahydrate ($Ni(NO_3)_2 \cdot 6H_2O$, CARLO ERBA, purity ≥ 98.5%) and ammonium perrhenate (NH_4ReO_4, Sigma-Aldrich Pte. Ltd., purity ≥ 99%) were used as the respective metal precursors for Ni and Re. Levulinic acid (Sigma-Aldrich Pte. Ltd., 98% purity) and 2-propanol (QREC Chemical, analytical reagent grade, >99%) were used as the reactant and solvent, respectively. All chemicals were of analytical grade and used as received.

2. Catalyst characterizations information

The textural properties of the calcined catalysts were characterized by N_2 adsorption–desorption measurements at −196 °C using a BELSORP Mini II gas sorption analyzer (MicrotracBEL, Japan). The specific surface area was calculated using the Brunauer–Emmett–Teller (BET) method, while the total pore volume and pore size distribution were derived from the desorption branch employing the Barrett–Joyner–Halenda (BJH) model. The actual metal loadings of the calcined samples were determined by inductively coupled plasma–optical emission spectroscopy (ICP–OES, PerkinElmer NexION® 2000) after complete acid digestion of the samples under microwave irradiation. The reducibility, hydrogen adsorption capacity, and surface acidity of the catalysts were investigated by temperature-programmed techniques using a Quantachrome TPRWin v4.10 analyzer. H_2 temperature-programmed reduction (H_2–TPR), H_2 temperature-programmed desorption (H_2–TPD), and NH_3 temperature-programmed desorption (NH_3–TPD) experiments were conducted following standard procedures as similar to previous experiments. [1] [2] The crystalline phases of both calcined and reduced catalysts were analyzed by X-ray diffraction (XRD) over a 2θ range of 10°–80° with a step time of 0.5 s. The structural evolution of the catalysts was examined by ex situ X-ray absorption spectroscopy (XAS) at Beamline 8 of the Synchrotron Light Research Institute (Thailand). Prior to XAS measurements, the reduced samples were diluted with boron nitride, pelletized, and analyzed in transmission mode at the Ni K-edge and Re L_3-edge, with corresponding metal foils used for energy calibration. The XAS data were processed using the ATHENA software package, and linear combination fitting (LCF) was employed to quantify the relative fractions of metallic and oxidized species. Wavelet transform

(WT) analyses were performed using the HAMA program with a Morlet wavelet over a k-range of 0–15 $Å^{-1}$ and an R-range of 0–6 Å. The surface chemical states of the catalysts were analyzed by X-ray photoelectron spectroscopy (XPS) using an AXIS SUPRA spectrometer (Kratos Analytical) equipped with a monochromatic Al Kα X-ray source. Prior to XPS measurements, the calcined samples were reduced ex situ at 600 °C for 3 h and subsequently passivated in 1% O_2/Ar for 1 h. Binding energies were calibrated against the C 1s peak at 284.6 eV, and spectral deconvolution was performed using XPSPEAK41 software. The morphology, particle size distribution, and lattice structure of the reduced catalysts were examined by a field emission scanning electron microscope (FE-SEM, JEOL JSM-7610FPLUS) and a transmission electron microscopy (TEM) coupled with energy-dispersive X-ray spectroscopy (EDS) using a JEOL JEM-3100F microscope operated at 300 kV. Finally, the thermal stability and coke deposition behavior of the reduced and spent catalysts were evaluated by thermogravimetric analysis (TGA) using a Mettler Toledo instrument (Switzerland).

Table S1 Summary of the XPS results obtained from the reduced Ni based catalysts.

Sample	Binding energy (eV)			Atomic concentration (%) [a]			Metallic fraction
	Ni 2*p*			Ni	Si	O	Ni [b] (0)
	Ni^0	Ni^{2+}	Sat.				
Ni-CS	852.5 869.4	856.3 874.1	861.9 880.5	1.74	21.02	77.23	0.15
Ni-IM-mSiO_2	852.9 869.8	856.1 873.8	862.1 880.5	1.85	28.32	69.82	0.20
Ni-IM-SiO_2	853.0 869.4	856.5 873.8	862.2 880.4	0.46	29.97	69.56	0.23
Ni-IM-MCM-41	852.9 869.2	856.2 873.5	862.2 880.4	2.65	28.31	69.03	0.27

[a] atomic concentration calculated from XPS survey; [b] Ni (0) fraction calculated from the ratio of Ni (0) / (Ni (0) + Ni (2+)).

Table S2 Summary of Ni composition (%) by LCF fitting from XANES data obtained from the reduced Ni based catalysts

Sample	Ni composition (%) by LCF fitting from XANES data	
	Ni^0	Ni^{2+}
Ni-CS	38	62
Ni-SiO_2-IMP	94	6
Ni-mSiO_2-IMP	93	7
Ni-MCM-41-IMP	94	6
$Ni_{12}Re_{1.63}$-CS	34	66
Used $Ni_{12}Re_{1.63}$-CS	70	30

Table S3 Summary of the XPS results obtained from the reduced Ni and Ni–Re based core-shell catalysts.

Sample	Binding energy (eV)							Atomic concentration (%) [a]				Metallic Fraction	
	Ni 2*p*			Re 4*f*				Ni	Re	Si	O	Ni [b] (0)	Re [c] (0)
	Ni^0	Ni^{2+}	Sat.	Re	Re^{4+}	Re^{6+}	Re^{7+}						
Ni-CS	852.5	856.3	861.9	-	-	-	-	1.74	-	21.02	77.23	0.15	-
	869.4	874.1	880.5	-	-	-	-						
$Ni_{12}Re_{0.78}$-CS	852.7	856.4	862.2	40.9	41.7	45.4	46.8	1.58	0.04	27.00	71.37	0.10	0.06
	869.3	873.9	880.4	42.7	43.8	48.4	49.8						
$Ni_{12}Re_{0.93}$-CS	852.6	856.3	862.3	40.9	41.6	45.4	46.8	1.14	0.01	25.71	73.13	0.13	0.10
	869.9	873.9	880.7	42.8	43.9	48.3	49.8						
$Ni_{12}Re_{1.63}$-CS	853.3	856.6	862.4	40.8	41.5	45.5	46.8	1.61	0.04	25.66	72.68	0.09	0.12
	869.5	874.1	880.9	42.8	43.9	48.3	49.6						
$Ni_{12}Re_{1.80}$-CS	852.5	856.5	862.1	40.8	41.3	45.4	46.8	2.12	0.01	25.67	72.19	0.06	0.09
	869.5	874.1	880.5	42.9	43.9	48.6	49.8						

[a] atomic concentration calculated from XPS survey; [b] Ni (0) fraction calculated from the ratio of Ni (0) / (Ni (0) + Ni (2+)); [c] Re (0) fraction calculated from the ratio of Re (0) / (Re (0) + Re (4+) + Re (6+) + Re (7+)).

Table S4 Catalytic performance comparison of Ni-based catalysts for levulinic acid (LA) hydrogenation to γ-valerolactone (GVL), highlighting LA conversion and GVL yield.

Entry	Catalyst	Metal content (wt%)	Solvent	T (°C)	time (h)	LA conv. (%)	GVL yield (%)	TOF (h^{-1})	TON	Rate (mmol GVL/g_{cat}^{-1} h^{-1}	Ref.
1	Ni_3-Zn_1@OMC	Ni:13.5 ,Zn: 5	Water	140	2	74	61	2.7	5.5	8.4	(Tang et al. 2023)[3]
2	Ni/Ru@WOMC	Ni: 9.6,Ru: 0.9	2-propanol	160	2	100	100	5.0	10.0	8.6	(Wang et al. 2023)[4]
3	30%Ni/O-clay450N	Ni: 26.31	1,4-Dioxane	140	5	100	100	1.3	6.4	5.7	(Kamble et al. 2023)[5]
4	Ni-Al	Ni: 53.30	Ethanol	140	2	100	97	4.5	9.1	41.2	(Shao et al. 2022)[6]
5	S3M1.5@NiPS-600	Ni: 24.3	Ethyl acetate, dodecane (internal standard)	150	3	95	91	1.9	5.7	7.9	(Li, Hsieh, and Lin 2022)[7]
6	1-Ni/C-400	Ni: 6.6	water	160	3	100	95	7.2	21.7	8.1	(Fang et al. 2019)[8]
7	500-NiFe NPs@C (3:1)	Ni: 14.95, Fe: 4.93	isopropanol	130	2	94	90	2.2	4.4	7.5	(Wang et al. 2018)[9]
8	Ni@FLG-600	Ni : 57.5	water (1,4-dioxane:internal standard)	130	7	99	99	0.2	1.3	1.8	(Zhang, Li et al. 2025)[10]
9	$NiRe_{0.075}/Al_2O_3$	Ni: 10.1 ,Re: 2.5	2-propanol	160	2	100	93	10.8	21.6	20.1	(Y. Maneewong et al. 2025)[1]
10	20Ni/ZAC-600	Ni : 49.7	H_2O	120	2	100	99.9	4.1	8.2	34.5	(X. Liu at al. 2025) [11]
11	NiRe-PS	Ni : 8.05	2-propanol	160	2	100	91.6	26.3	52.7	39.4	(Y. Maneewong & P. Lakhani et al. 2026)[2]
12	$Ni_{12}Re_{1.63}$-CS	Ni : 12.8,Re: 1.63	2-propanol	160	2	43.4	40.3	15.3	30.6	34.7	This work
13	$Ni_{12}Re_{1.63}$-CS	Ni : 12.8,Re: 1.63	2-propanol	180	2	92.6	91.2	34.5	69.1	78.5	This work
14	$Ni_{12}Re_{1.63}$-CS	Ni : 12.8,Re: 1.63	2-propanol	200	2	100	94.4	35.8	71.5	81.3	This work

Table S5 Summary of the XPS results obtained from the used catalysts.

Sample	Binding energy (eV)							Atomic concentration (%) [a]				Metallic Fraction	
	Ni 2*p*			Re 4*f*				Ni	Re	Si	O	Ni [b] (0)	Re [c] (0)
	Ni^0	Ni^{2+}	Sat.	Re	Re^{4+}	Re^{6+}	Re^{7+}						
Reduced $Ni_{12}Re_{1.63}$-CS	853.3	856.6	862.4	40.8	41.5	45.5	46.8	1.61	0.04	25.66	72.68	0.09	0.12
	869.5	874.1	880.9	42.8	43.9	48.3	49.6						
Used $Ni_{12}Re_{1.63}$-CS	852.2	856.2	861.9	-	-	45.2	46.8	0.89	0.01	26.34	72.75	0.13	0.12
	869.5	874.2	880.7	42.7	43.8	48.5	49.8						

[a] atomic concentration calculated from XPS survey; [b] Ni (0) fraction calculated from the ratio of Ni (0) / (Ni (0) + Ni (2+));

[c] Re (0) fraction calculated from the ratio of Re (0) / (Re (0) + Re (4+) + Re (6+) + Re (7+))

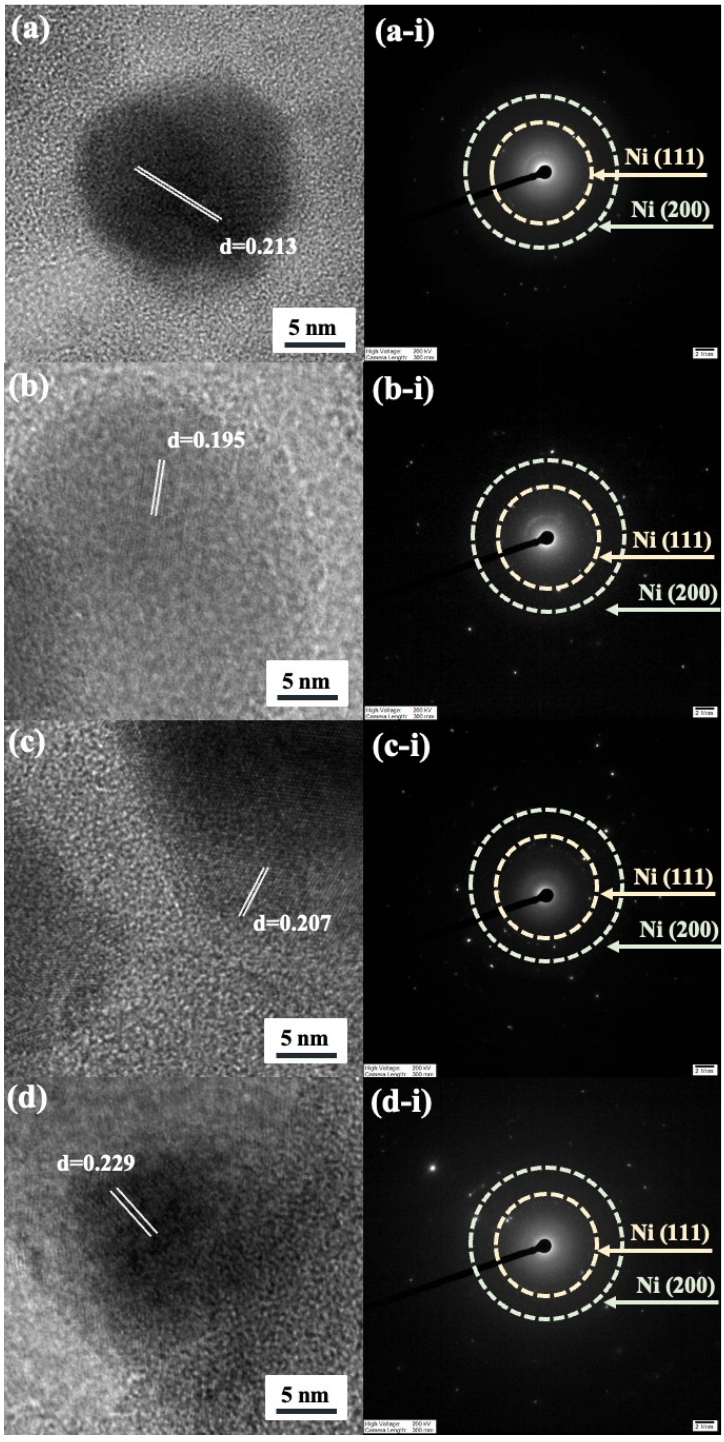

Fig. S1 (a to d) high-resolution TEM (HR-TEM) images and (a-i to d-i) diffraction pattern of the reduced (a and a-i) Ni-CS, (b and b-i) Ni-IM-mSiO_2, (c and c-i) Ni-IM-SiO_2, and (d and d-i) Ni-IM-MCM-41 catalysts, respectively.

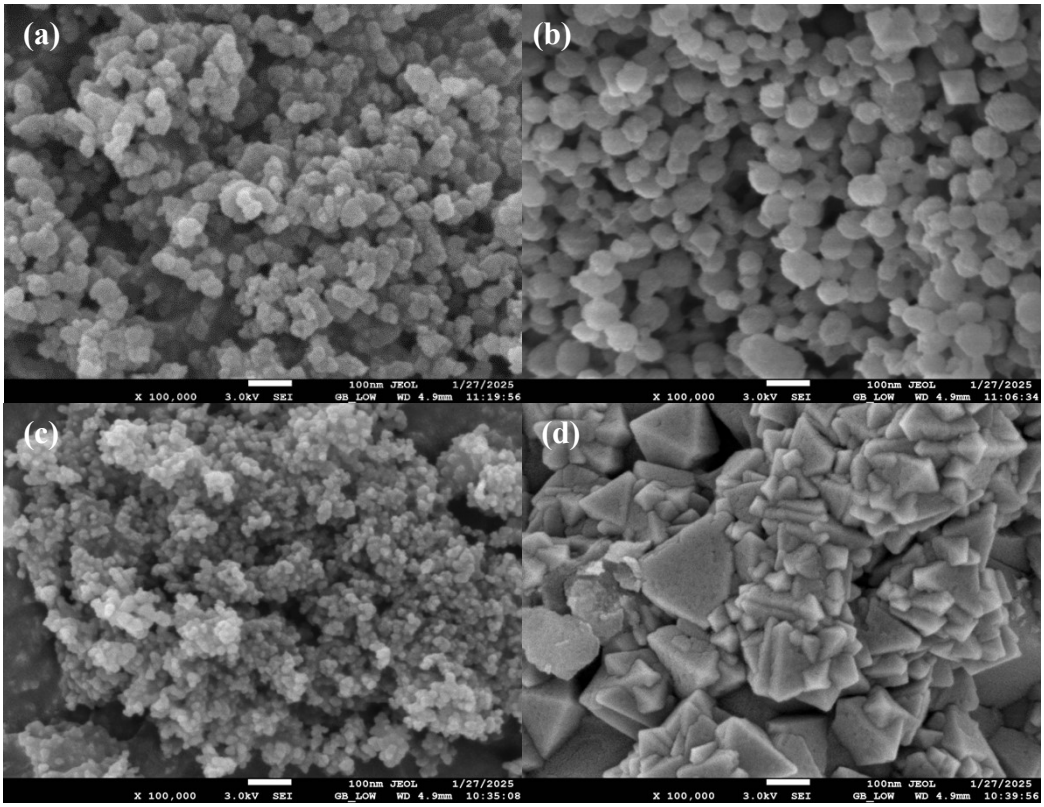

Fig. S2 (a to d) Field Emission Scanning Electron Microscope (FE-SEM) images of the calcined (a) Ni-CS, (b) Ni-IM-mSiO_2, (c) Ni-IM-SiO_2, and (d) Ni-IM-MCM-41 catalysts.

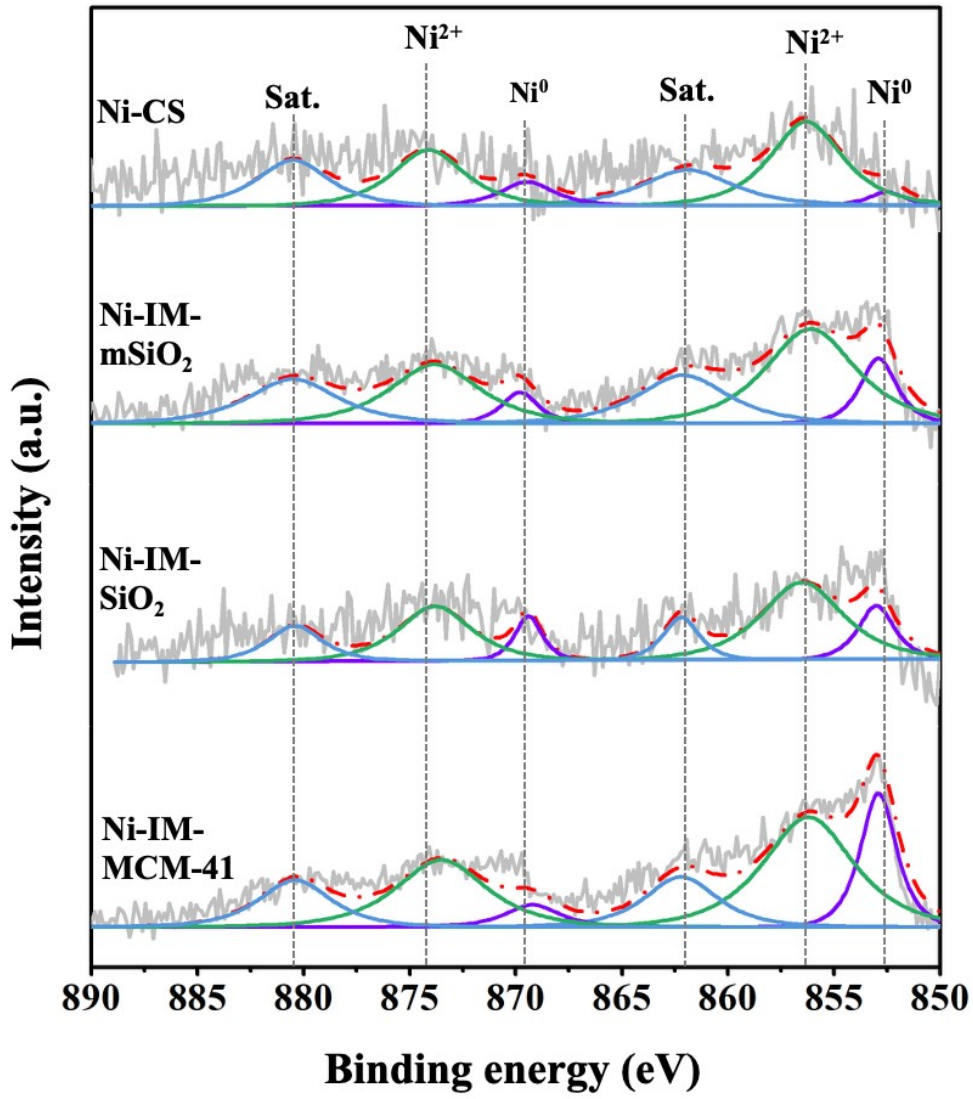

Fig. S3 X-ray photoelectron spectroscopy (XPS) Ni 2*p* spectra of reduced and passivated Ni-CS, Ni-IM-mSiO_2, Ni-IM-SiO_2, and Ni-IM-MCM-41 catalysts

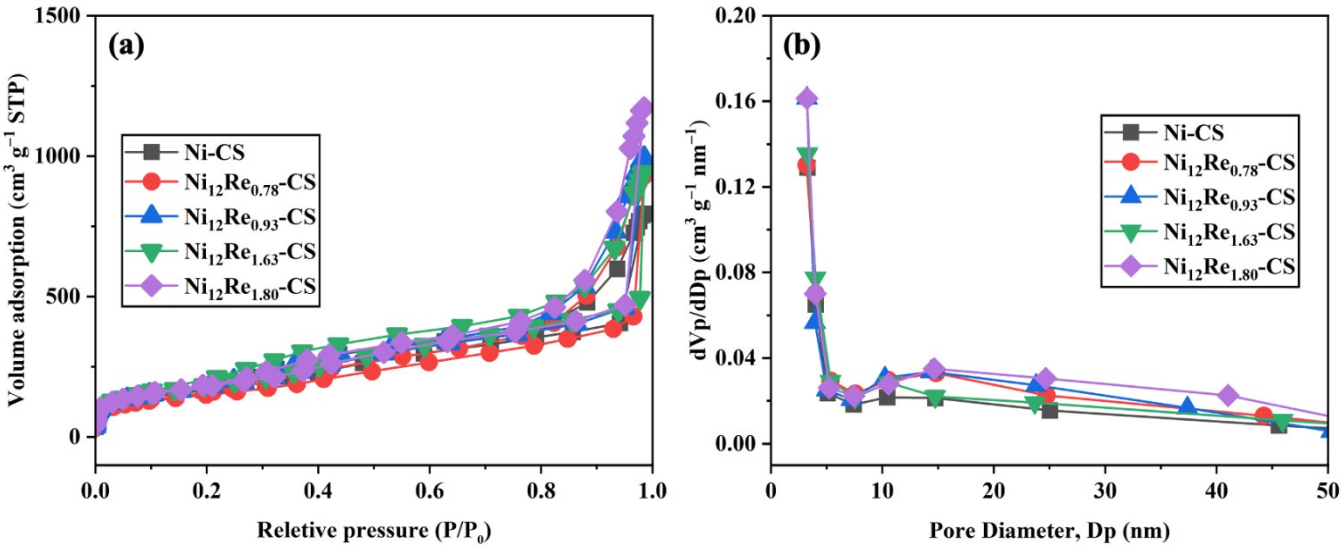

Fig. S4 (a) N_2 adsorption–desorption isotherms and (b) pore size distribution derived from the BJH model for the calcined Ni-CS $Ni_{12}Re_{0.78}$-CS, $Ni_{12}Re_{0.93}$-CS, $Ni_{12}Re_{1.63}$-CS, and $Ni_{12}Re_{1.80}$-CS catalysts.

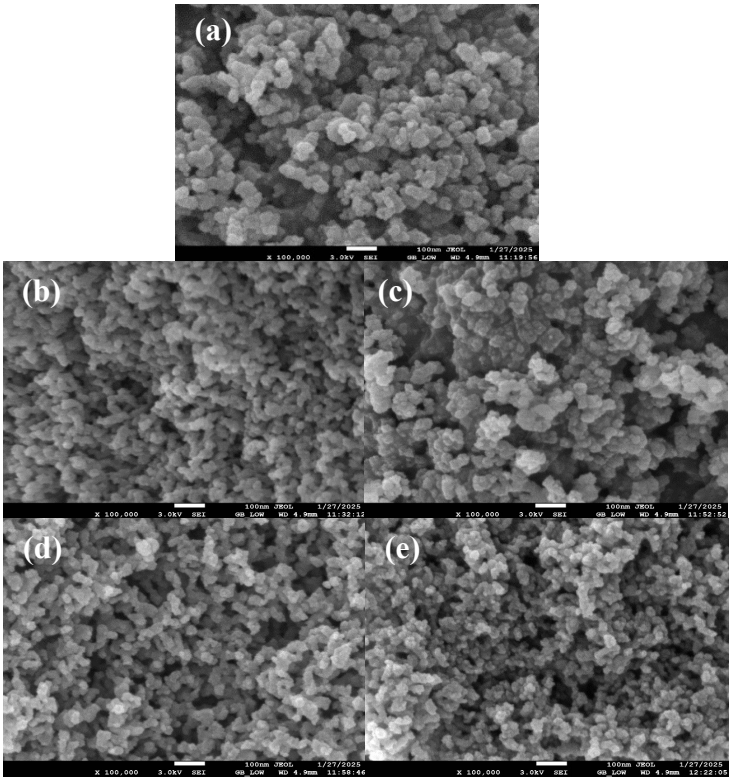

Fig. S5 (a to d) Field Emission Scanning Electron Microscope (FE-SEM) images of the calcined (a) Ni-CS (b) $Ni_{12}Re_{0.78}$-CS, (c) $Ni_{12}Re_{0.93}$-CS, (d) $Ni_{12}Re_{1.63}$-CS, and (e) $Ni_{12}Re_{1.80}$-CS catalysts.

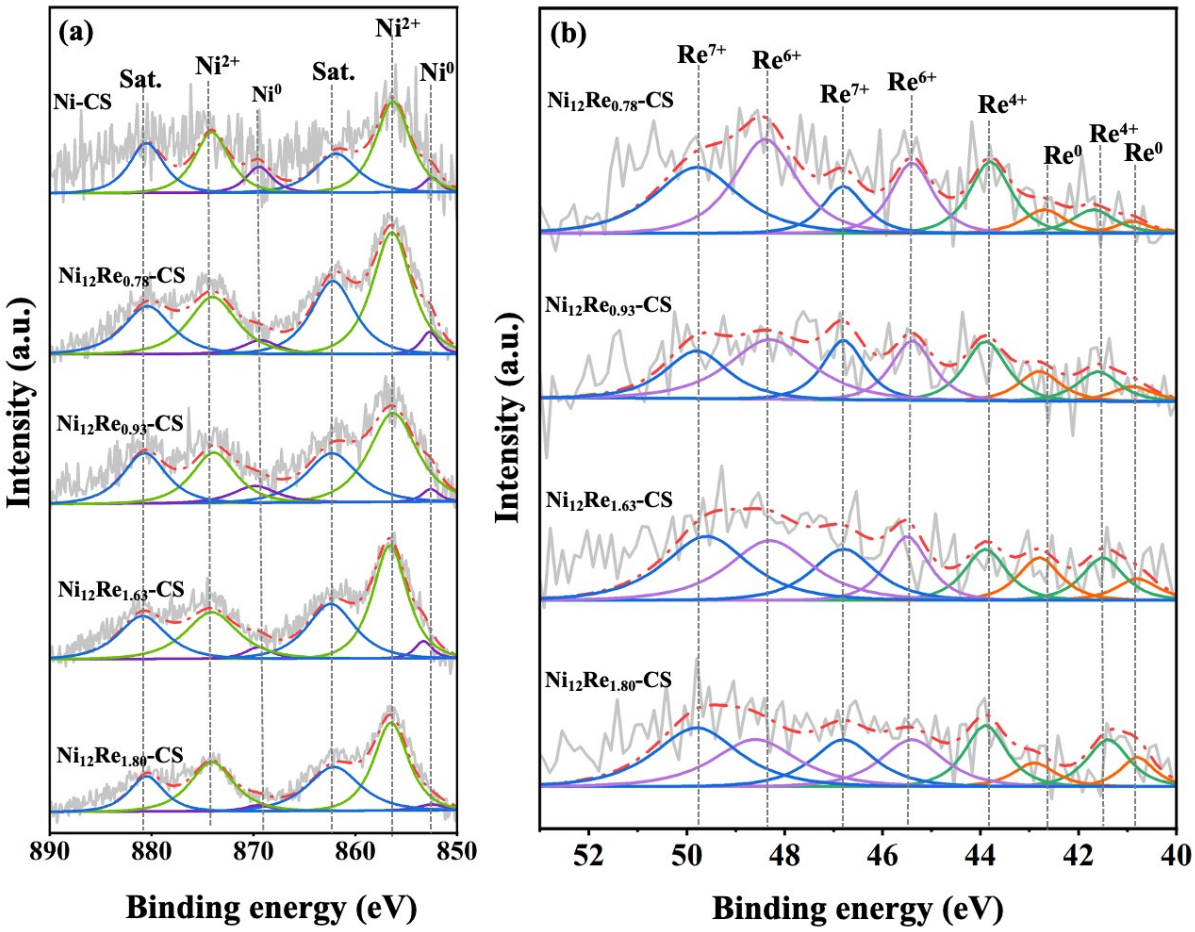

Fig. S6 X-ray photoelectron spectroscopy (XPS) (a) Ni 2*p* and (b) Re 4*f* spectra of reduced and passivated Ni-CS, $Ni_{12}Re_{0.78}$-CS, $Ni_{12}Re_{0.93}$-CS, $Ni_{12}Re_{1.63}$-CS, and $Ni_{12}Re_{1.80}$-CS catalysts.

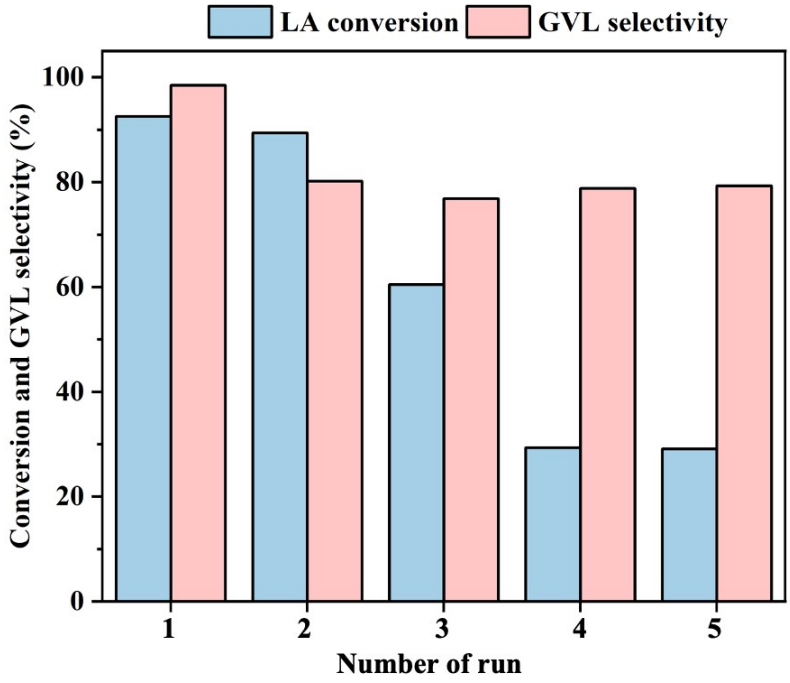

Fig. S7 Reusability of $Ni_{12}Re_{1.63}$-CS catalyst at a reaction temperature of 180 ˚C, 2h, 10 bar of H_2 pressure, 0.025 g catalyst, LA 0.5 g, and 2-PrOH (20 ml)

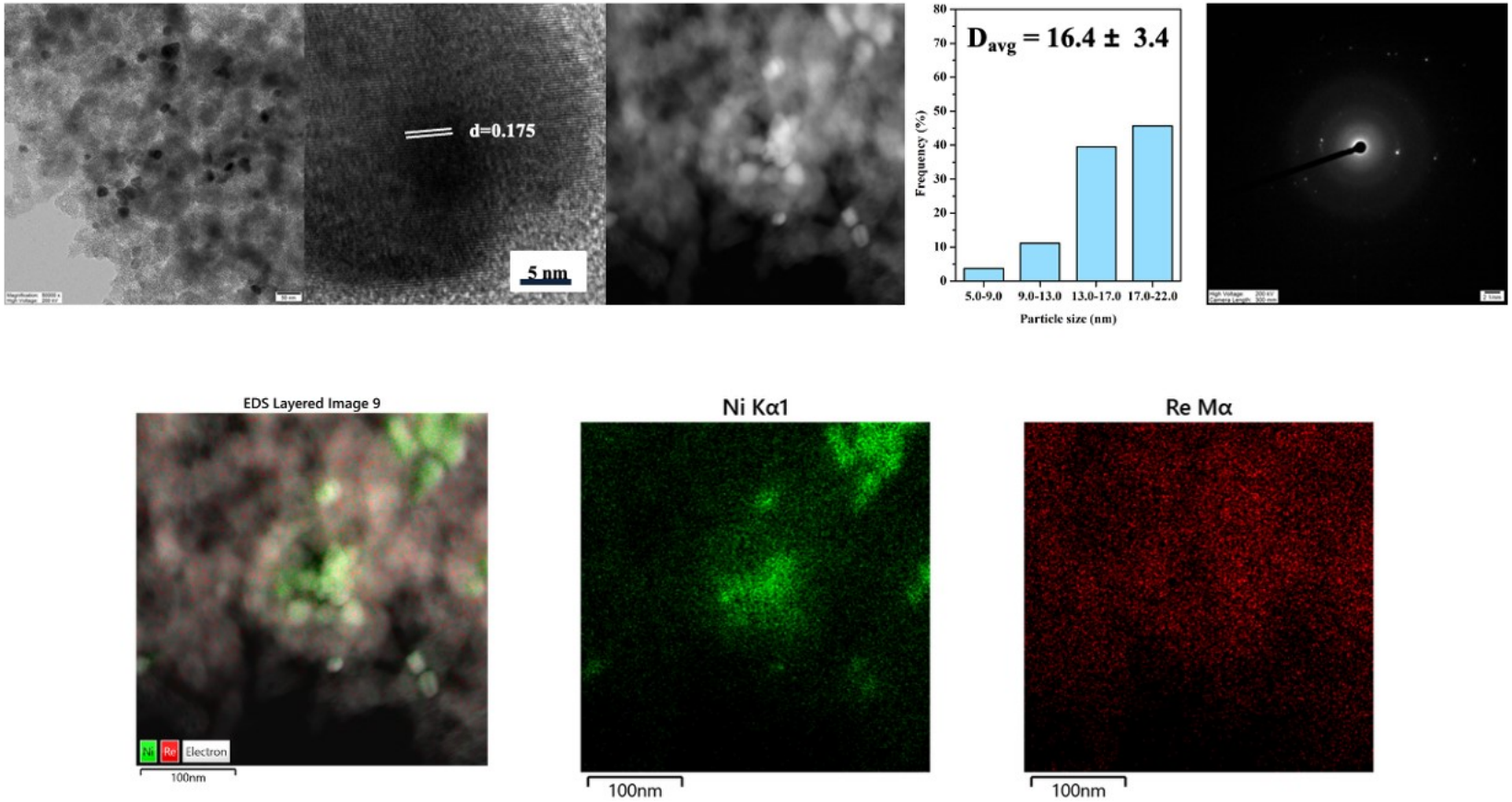

Fig. S8 TEM image of used $Ni_{12}Re_{1.63}$-CS catalyst

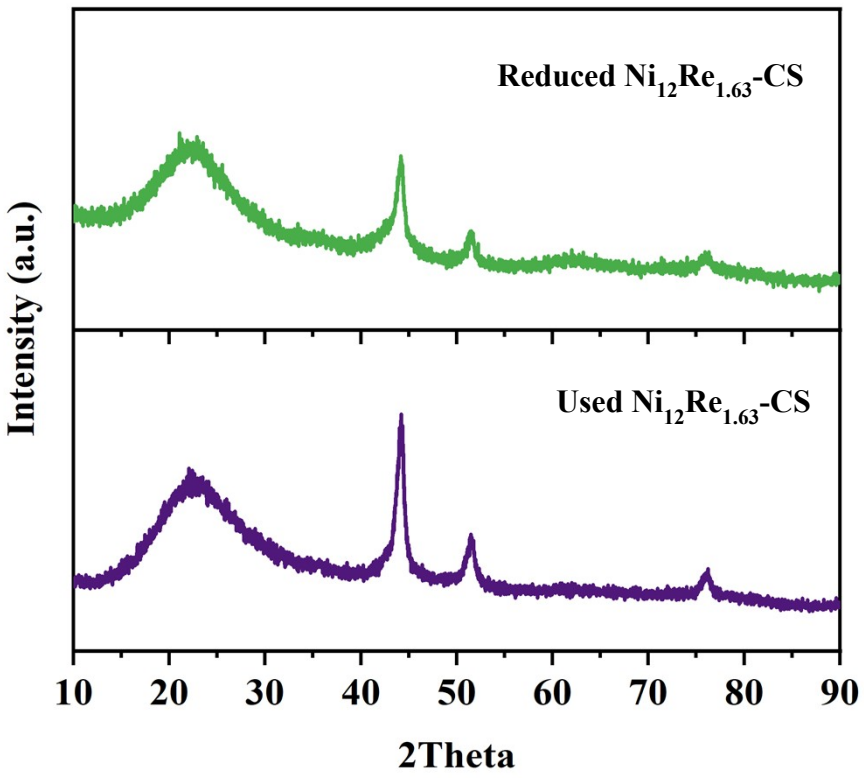

Fig. S9 XRD comparison of reduced and used $Ni_{12}Re_{1.63}$-CS catalyst

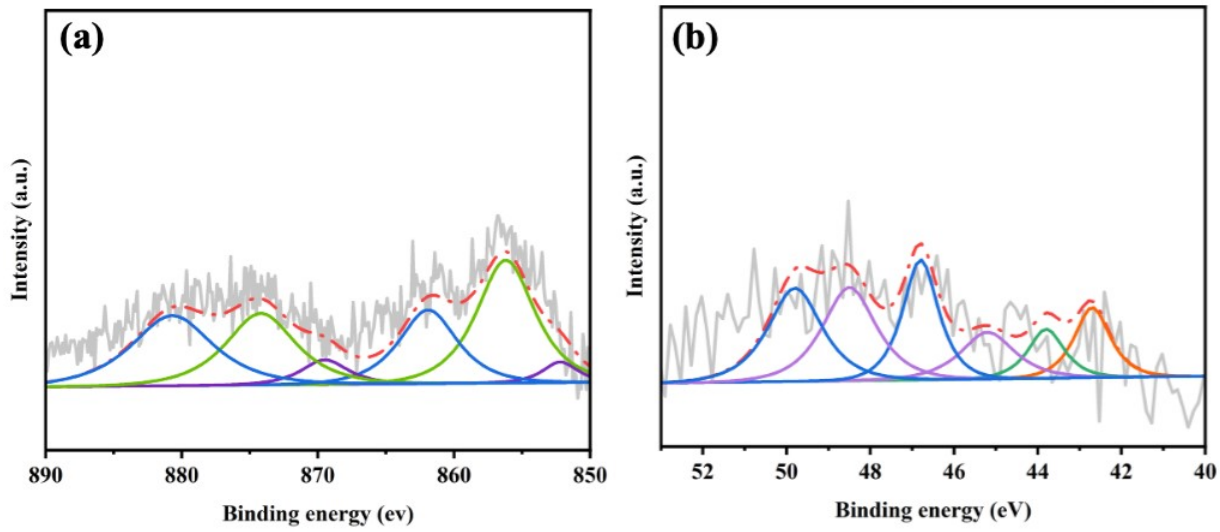

Fig. S10 X-ray photoelectron spectroscopy (XPS) (a) Ni 2*p* and (b) Re 4*f* spectra of used $Ni_{12}Re_{1.63}$-CS catalyst

.

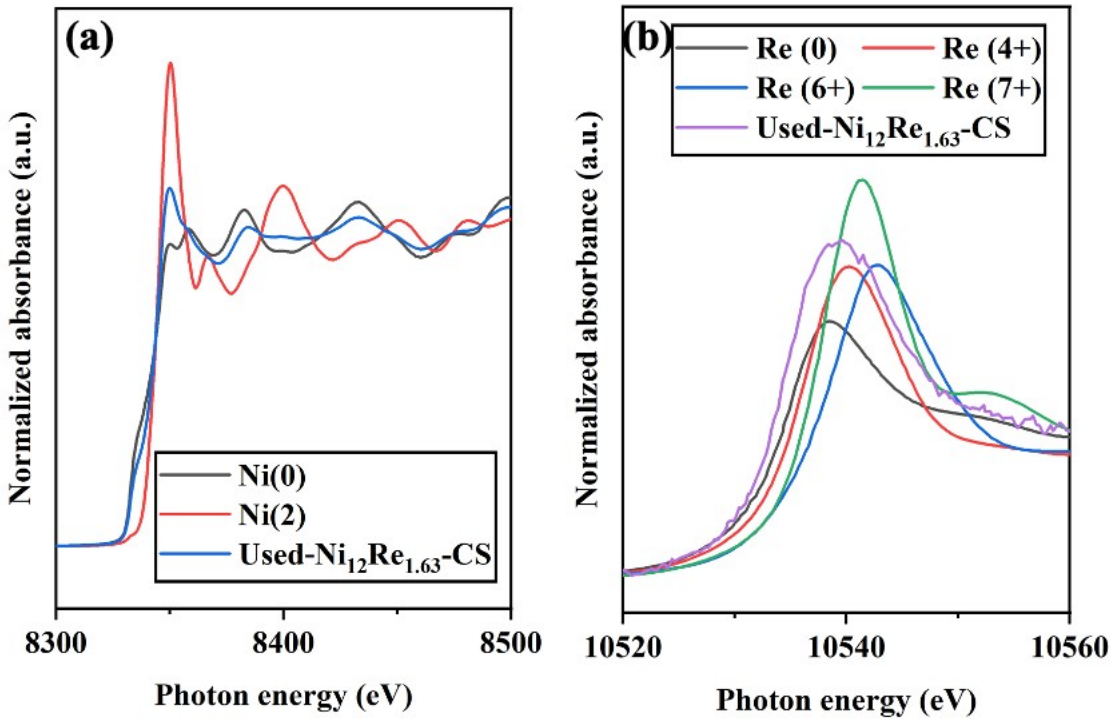

Fig. S11 Normalized (a) Ni K- and (b) Re L_3-edges XANES spectra of used $Ni_{12}Re_{1.63}$-CS catalyst

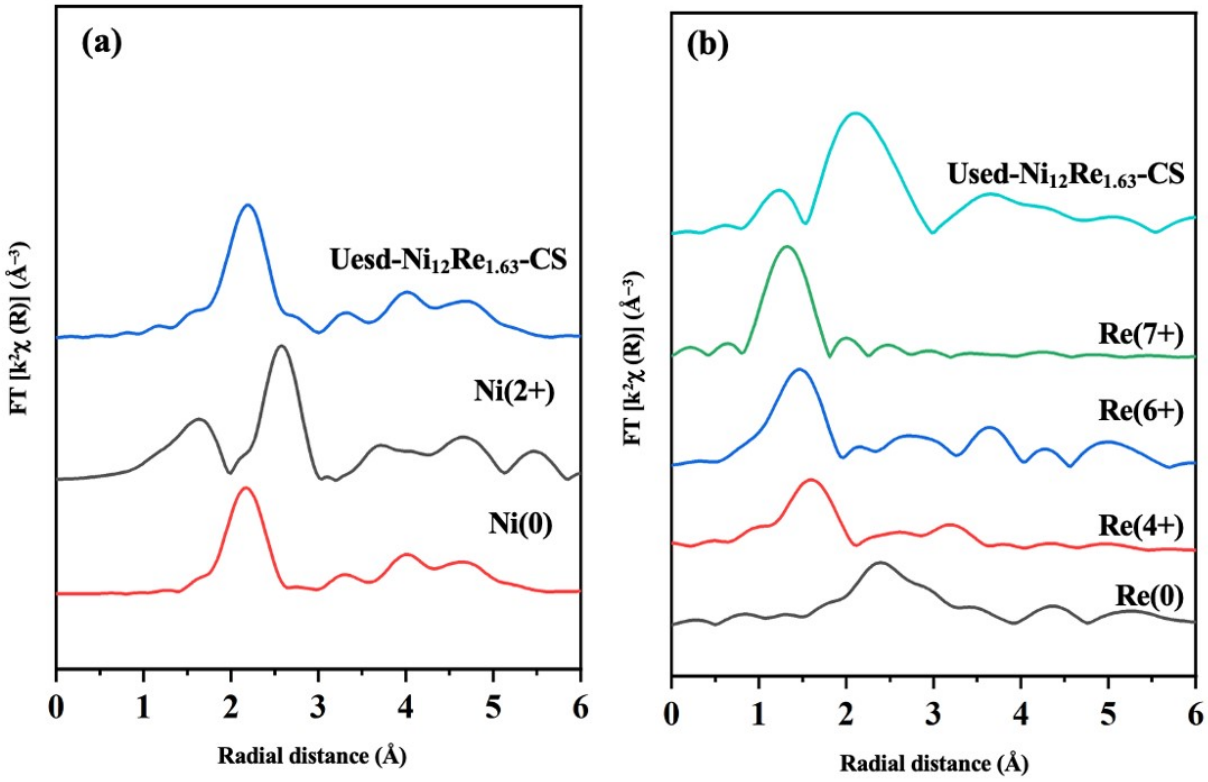

Fig. S12 EXAFS spectra at the (a) Ni K-edge and (b) Re L_3-edge for the used $Ni_{12}Re_{1.63}$-CS catalyst

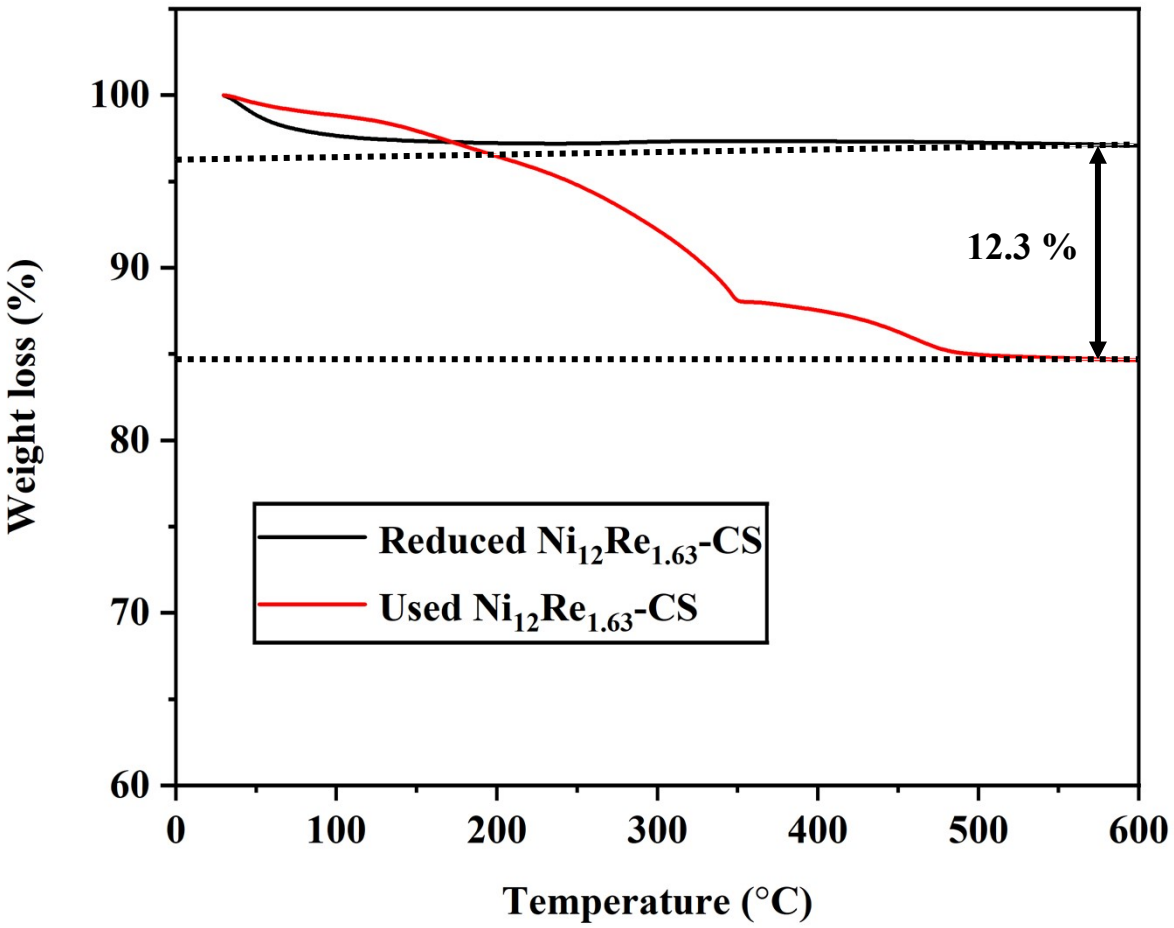

Fig. S13 TGA comparison of reduced and used $Ni_{12}Re_{1.63}$-CS catalyst

References

1. Y. Maneewong, P. Nimmanterdwong, S. Ratchahat, C. Sakdaronnarong, W. Limphirat, P. Khemthong, B. Rungtaweevoranit, K. Faungnawakij, S. Assabumrungrat and Y.-C. Lin, *Chemical Engineering Journal*, 2025, **508**, 160969.
2. Y. Maneewong, P. Lakhani, S. Ratchahat, C. Sakdaronnarong, W. Limphirat, B. Rungtaweevoranit, S. Assabumrungrat, K. Khosukwiwat, K. Choojun and T. Sooknoi, *Green Chemistry*, 2026.
3. Y. Tang, J. Fu, Y. Wang, H. Guo and X. Qi, *Fuel Processing Technology*, 2023, **240**, 107559.
4. X. Wang, X. Qi, M. Qiu, F. Shen, J. Yang and B. Shen, *Fuel*, 2023, **341**, 127720.
5. P. A. Kamble, C. Vinod, V. K. Rathod and M. L. Kantam, *Catalysis Today*, 2023, **408**, 36-49.
6. Y. Shao, K. Sun, M. Fan, J. Wang, G. Gao, L. Zhang, S. Zhang and X. Hu, *Chemical Engineering Science*, 2022, **248**, 117258.
7. C.-C. Li, C.-H. Hsieh and Y.-C. Lin, *Molecular Catalysis*, 2022, **523**, 111720.
8. S. Fang, Z. Cui, Y. Zhu, C. Wang, J. Bai, X. Zhang, Y. Xu, Q. Liu, L. Chen and Q. Zhang, *Journal of Energy Chemistry*, 2019, **37**, 204-214.
9. H. Wang, C. Chen, H. Zhang, G. Wang and H. Zhao, *Chinese Journal of Catalysis*, 2018, **39**, 1599-1607.
10. Y. Zhang, Y. Li, C. Shen, C. Yang, H. Wu, C. Jiang, S. Chen, M. Li, Y. Li and W. Ding, *Applied Catalysis B: Environment and Energy*, 2025, **361**, 124595.
11. X. Liu, D. Han, J. Xia, D. Yan, R. Diao, F. Qi, Z. Wang, L. Yang, X. Wu, P. Ma and Y. Zhang, *Journal of Materials Chemistry A*, 2025, **13**, 20924-20933.